



The ASC Speck and NLRP3 Inflammasome Function Are Spatially and Temporally Distinct

Abhinit Nagar, Tabassum Rahman and Jonathan A. Harton*

Department of Immunology & Microbial Disease, Albany Medical College, Albany, NY, United States

Although considered the ternary inflammasome structure, whether the singular, perinuclear NLRP3:ASC speck is synonymous with the NLRP3 inflammasome is unclear. Herein, we report that the NLRP3:ASC speck is not required for nigericin-induced inflammasome activation but facilitates and maximizes IL-1 β processing. Furthermore, the NLRP3 agonists H₂O₂ and MSU elicited IL-1 β maturation without inducing specks. Notably, caspase-1 activity is spatially distinct from the speck, occurring at multiple cytoplasmic sites. Additionally, caspase-1 activity negatively regulates speck frequency and speck size, while speck numbers and IL-1 β processing are negatively correlated, cyclical and can be uncoupled by NLRP3 mutations or inhibiting microtubule polymerization. Finally, when specks are present, caspase-1 is likely activated after leaving the speck structure. Thus, the speck is not the NLRP3 inflammasome itself, but is instead a dynamic structure which may amplify the NLRP3 response to weak stimuli by facilitating the formation and release of small NLRP3:ASC complexes which in turn activate caspase-1.

Keywords: speck, NLRP3, inflammasome, caspase-1, colchicine, IL-1 β , nigericin, H₂O₂

OPEN ACCESS

Edited by:

Akihiko Yoshimura,
Keio University, Japan

Reviewed by:

Hideki Hara,
Keio University, Japan
Junya Masumoto,
Ehime University, Japan

*Correspondence:

Jonathan A. Harton
hartonj@amc.edu

Specialty section:

This article was submitted to
Inflammation,
a section of the journal
Frontiers in Immunology

Received: 03 August 2021

Accepted: 23 September 2021

Published: 21 October 2021

Citation:

Nagar A, Rahman T and
Harton JA (2021) The ASC Speck
and NLRP3 Inflammasome
Function Are Spatially and
Temporally Distinct.
Front. Immunol. 12:752482.
doi: 10.3389/fimmu.2021.752482

INTRODUCTION

Inflammasomes are intracellular, multiprotein complexes that assemble and activate caspase-1 following stimuli of microbial, host, and environmental origin (1, 2). Active caspase-1 cleaves pro-IL-1 β and pro-IL-18, cytokines vitally important during infection and inflammation (3, 4). Caspase-1 also cleaves gasdermin-D (GSDMD) which then forms a membrane pore facilitating IL-1 β release and pyroptotic cell death (5). Most inflammasomes comprise members of the NLRP family of intracellular pathogen receptors that associate with the ASC adaptor protein to recruit caspase-1 (1, 3, 4). Among NLRP inflammasomes, the NLRP3 inflammasome is essential for innate protection against a plethora of microbial pathogens and contributes to numerous inflammatory pathologies (1, 3).

ASC-dependent inflammasome activation is accompanied by rapid relocation of the NLR and ASC into a singular, perinuclear, punctate “speck” structure of approximately 1 μ m (6, 7). The speck is thought to act as a supramolecular signaling complex (SMOC), higher-order structures which locally concentrate weakly interacting proteins required for signal transduction (8–10). Speck formation is rapid causing a concomitant drop in cytosolic ASC concentration, approximately 200-fold, to submicromolar concentrations within 100 s (2), and almost all available NLRP3 and ASC

oligomerize within minutes (11). Speck assembly is microtubule-dependent (12–14). During NLRP3 inflammasome activation, ASC binds to damaged mitochondria and is drawn *via* microtubules to NLRP3 on the endoplasmic reticulum (13). NLRP3 and ASC then associate forming the speck (13, 15). Accordingly, microtubule depolymerization agents such as colchicine block speck formation (12) and impair NLRP3 inflammasome maturation of IL-1 β induced by monosodium urate crystals (16). Thus, colchicine is a drug of choice for treating gout, an NLRP3-related inflammatory condition (17).

Since NLRP inflammasome activity and speck assembly are concomitant and both require interaction between the NLRP and ASC, NLRP3:ASC specks are generally equated with the inflammasome (13). Studies using small molecules including colchicine, nocodazole, and others which prevent both speck assembly and inflammasome function support this view (12, 18). However, biochemical analysis suggests that active NLRP1:ASC: caspase-1 complexes may be less than ~ 0.45 μm in diameter (~ 700 kDa) (19), values generally accepted for NLRP3 complexes as well (20) and are much smaller than the 1- μm speck structure. Likewise, *in vitro*-assembled NLRP1 (15 Å) and NLRP3 (100 nm), inflammasome structures have an approximately 100–1,000-fold smaller diameter than the speck, different arrangements, and distinct stoichiometries (20, 21). Furthermore, while NLRP3:ASC speck formation requires a few minutes, IL-1 β processing is detected within 1 h (22). Such size, stoichiometric, and temporal disparities between the speck and the inflammasome suggest that these structures may have distinct functions. Nevertheless, the relationship between the inflammasome and the speck is still unclear. Whether such distinctions reflect separate functions for the speck and inflammasome is unanswered.

This study establishes that NLRP3-mediated caspase-1 activity (the inflammasome) is distinct and independent of the NLRP3:ASC speck. While not required and insufficient for NLRP3 inflammasome function, the NLRP3:ASC speck is a dynamic, spatially, and temporally distinct structure regulated in part by caspase-1. Furthermore, the speck lowers the NLRP3 inflammasome activation threshold, potentially amplifying the formation and release of much smaller inflammasome complexes. The implications of our data and the relationship between ASC speck structures and the NLRP3 inflammasome are discussed.

MATERIALS AND METHODS

Cell Culture

Human kidney epithelial cells (HEK293T) (ATCC; Cat. # CRL-11268) and immortalized bone marrow-derived macrophages (iBMDMs) (a gift from Dr. Katherine Fitzgerald, UMass Medical School, Worcester, MA) were cultured in complete Dulbecco's modified Eagle's medium/high glucose (DMEM) (HyClone™; Cat. # SH30022.01) supplemented 10% FBS (Atlanta Biologicals; Cat. # S11050), 1 \times GlutaMAX (Gibco; Cat. # 35050-061), and 0.1% penicillin/streptomycin at 37°C, 5% CO₂. Primary human

monocytes were obtained from the University of Nebraska Medical Center and cultured in DMEM supplemented with 10% human AB serum (Corning; Cat. # 35-060-Cl). THP-1 (ATCC; TIB-202) monocytic cells were cultured in RPMI-1640 (HyClone™; Cat. # SH30027.01) supplemented with 10% FBS, 1 \times β -mercaptoethanol (Gibco; Cat. # 21985) and 1 \times GlutaMAX. THP-1 cells were differentiated to macrophages by treatment with phorbol 12-myristate 13-acetate (PMA) (100 nM) for 72 h. Cultured cell lines were maintained at subconfluence and split every 2–3 days. Cell numbers and viability were determined by trypan blue exclusion.

Expression Plasmids, Construct, and DNA Transfection

Expression plasmids encoding NLRP3, NLRP3 cysteine mutants, and chimeric NLRP3 mutants, myc-ASC, GFP-ASC, caspase-1 (CASP1), and pro-IL-1 β (IL1B) have been described previously (23–25). GFP-YVAD was PCR-amplified from pEGFP-C3 and cloned into the Lamp1-RFP plasmid (a gift from Walter Mothes; RRID: Addgene Cat. # 1817) (26) as an *EcoRI* [New England Biolabs (NEB); Cat. # R0101S]/*BamHI* (NEB; Cat. # R0136S) fragment to generate GFP-YVAD-RFP (**Supplementary Figure S1**). Ligation was performed using T4 DNA ligase (Promega; Cat. # M1801) using the protocol of the manufacturer for staggered end ligation. Caspase-1 mutants (**Supplementary Figure S2A**) were generated by QuikChange PCR. The parental caspase-1 plasmid (methylated) was digested using *DpnI* (NEB; Cat. # R0176S). Plasmids were transformed in *Escherichia coli* DH5 α -competent cells (NEB; Cat. # C29871). All site-directed changes were confirmed by sequencing. Oligonucleotide primers used in this project were produced by Integrated DNA Technology and are listed in **Table 1**. DNA transfections were carried out using FuGENE6 (2.5 $\mu\text{l}/\mu\text{g}$ DNA) (Roche Applied Science; Cat. # 11988387001) as per the protocol of the manufacturer.

Transfection Conditions

For assays of stimulus-dependent NLRP3-inflammasome IL-1 β maturation and release (inflammasome reconstitution), HEK293T cells were seeded (2.5×10^4 cells/well/ml) in 24-well plates, cultured overnight, and transfected with 40 ng CASP1, 200 ng IL1B, 8 ng ASC, and 100 ng of either an NLR or control (pcDNA3) plasmid. Under these conditions, specks are not evident and NLRP3 and ASC cannot be detected by immunofluorescence staining due to low levels of expression.

Observing macrophage-like, agonist-dependent speck formation in HEK293T cells either alone [using time-of-flight inflammasome evaluation (TOFIE)] or in conjunction with caspase-1 activity [using inflammasome and caspase-1 activity characterization and evaluation (ICCE)] requires higher levels of expressed NLRP3 and ASC. HEK293T cells (2×10^5) were seeded per well/ml in 12-well plates and, after overnight incubation, transfected with 100 ng NLRP3, 50 ng GFP-ASC, and either alone or with caspase-1 (20 or 50 ng). The empty vector, pcDNA3, was used to adjust the final amount of DNA to 1 μg prior to transfection.

For the evaluation of speck formation capacity by microscopy, 5×10^5 HEK293Ts were seeded per well/ml in

TABLE 1 | Primers used in the study.

Primer name (purpose)	Sequence
hCaspase-1 D103N (mutate D103 to N)	For: 5'-GAAGAAAGTACTCCTTGAGAGTTTTGCATATTAAGGTAATTTCCA-3' Rev: 5'-TGGAAATTACCTTAATATGCAAACTCTCAAGGAGTACTTTCTTC-3'
hCaspase-1 D119N (mutate D119 to N)	For: 5'-GCATAGCTGGGTTGTTCTGCACTGCCTGAGG-3' Rev: 5'-CCTCAGGCAGTGCAGAACAACCCAGCTATGC-3'
hCaspase-1 D297N (mutate D297 to N)	For: 5'-CCAGAACTCCTACTGAATTTTTAAACACACACACACC-3' Rev: 5'-GGTGTGGTGTGGTTTAAAAATTCAGTAGGAGTTTCTGG-3'
hCaspase-1 D314/315N (mutate D314/315 to N)	For: 5'-GTGGGCTTTCTTAATAGCATTATTTCTCAAACCTTCTGTAGTTG-3' Rev: 5'-CAACTACAGAAGAGTTTGAGAATAATGCTATTAAGAAAGCCAC-3'
hCaspase-1 DEAD (mutate C285 to A)	For: 5'-GCTGTACCACGGGCGCCTGGATGATG-3' Rev: 5'-CATCATCCAGGCCGCCGTGGTGACAGC-3'
GFP-EcoRI/BamHI (clone GFP in LAMP1-RFP)	For: 5'-CCCAAGCCAGGAAGGGGCAGGTTTCAGATAATGCACGTGTTT-3' Rev: 5'-CCTATGGATCCATCAGCTACATACTTGACAGCTCGTCCATGCCAG-3'
GFP-YVAD-RFP (introduction of YVAD to GFP-RFP construct)	For: 5'-CTGATGGATCCACGGCGCCACCATGGCCTCC-3' Rev: 5'-GGAGGCCATGGTGGCGCCGTGGATCCATCAG-3'

six-well plates with coverslips, after overnight incubation, transfected with 1 μ g NLRP3 or its chimeric mutants and 1 μ g ASC, and incubated for 20 h.

FRET and Caspase-1 Activation Assay

The specificity of caspase-1 is significantly increased if peptide flanking the caspase-1-specific sequence YVAD is increased by only four amino acid sequences (27). Thus, a double reporter (GFP-YVAD-RFP) construct with the sequence "YVAD" separating GFP and RFP was generated, which is expected to have higher specificity than FLICA (**Supplementary Figure S1**). HEK293Ts (2×10^5) were seeded per well/ml in 12-well plates, after overnight incubation, and transfected with 100 ng NLRP3, 100 ng GFP-ASC, 400 ng CASP1 (WT or mutant), and GFP-YVAD-RFP. As a positive control for FRET, cells were transfected with all the above stated plasmids except caspase-1, and for negative control, cells were transfected with GFP and RFP expressed on different plasmids instead of GFP-YVAD-RFP expressing plasmid. Transfections were carried out at a constant DNA concentration of 1 μ g/well. The empty vector, pcDNA3, was used to adjust the final amount of DNA to 1 μ g. After overnight incubation, cells were either analyzed by microscopy to evaluate the distribution of GFP-YVAD-RFP reporter. To measure caspase-1 activation using FRET, cells were harvested after overnight incubation and fixed using 4% paraformaldehyde (PFA) as described above. The cells were acquired on LSRII flow cytometer equipped with 405, 488, and 642 nm lasers with long-pass filter of 505 nm and band-pass filters of 450/50, 530/30, and 660/20 nm. Acquisition was done using BD FACSDiva software. Data were analyzed using FlowJo. Samples were gated to exclude debris and cell doublets. Singlet population was further gated for GFP staining. A stop gate of 10^4 cells was set on the GFP-positive gate. GFP+ cells were plotted for RFP versus GFP staining. Since the flow cytometer lacked lasers to excite RFP, only the source for RFP signal was through GFP emission leading to FRET. Thus, events in FRET channel were normalized to 100 for the GFP-YVAD-RFP-transfected sample and normalized to 0 for the GFP+RFP-transfected samples. FRET was calculated using the following formula:

$$\% \text{ FRET} = \frac{\% \text{ Events (FRET: Sample)} - \% \text{ Events (FRET: GFP + RFP)}}{\% \text{ Events (FRET: GFP - YVAD - RFP)} - \% \text{ Events (FRET: GFP + RFP)}}$$

For caspase-1 activity measurements, the caspase-1-transfected sample was normalized to 100 and the GFP-YVAD-RFP-alone-transfected sample was normalized to 0. Caspase-1 activity was measured using the following formula:

$$\% \text{ Caspase - 1 activity} = \frac{100 - \% \text{ FRET(Sample)}}{100 - \% \text{ FRET(Caspase - 1)}}$$

Inflammasome Activation

Inflammasome-reconstituted HEK293T cells were infected with *Francisella novicida* U112 (Albany Medical College Microbiology Core Facility) at an moi of 100, 4 h post-transfection. After 24 h, culture supernatants were collected by centrifugation. For H₂O₂ (Sigma Aldrich; Cat. # 216713), nigericin (Invivogen; Cat. # tlr1-nig), and monosodium urate (MSU) (Sigma Aldrich; Cat#U-2875) stimulation, reconstituted HEK293T cells were treated 18 h post-transfection with 100 μ M H₂O₂ for 1 h, with 5 μ M nigericin for 2 h or with 150 μ g/ml MSU for 2 h, and culture supernatants were collected. Control untreated wells were harvested at the same time. Secreted IL-1 β was measured with the Human IL-1 β cytosol ELISA (Invitrogen; Cat. # CHC1213) as per the instructions of the manufacturer. THP-1 cells, immortalized BMDMs, and primary human monocytes were treated with 100 ng/ml LPS (O26:B6) (Sigma Aldrich; Cat. # L2654) for 3–4 h. Following LPS treatment, cells were stimulated with 5 mM ATP (Sigma Aldrich; Cat. # A3377) or 10 μ M nigericin for 30 min or 150 μ g/ml MSU for 2 h. For microscopy, THP-1 cells were treated with 100 nM PMA for 72 h, washed, and then supplemented with 500 μ l serum-free RPMI media containing vehicle or 5 μ M colchicine. After 1 h, cells were stimulated with 500 μ l serum-free RPMI media containing nigericin.

Time-of-Flight Inflammasome Evaluation

A portion of the samples prepared for ImageStream[®]X Mark II (ISXII) analysis (below) was diluted to 200 μ l in ISXII cell suspension buffer and acquired on an LSRII flow cytometer

equipped with 405, 488, and 642 nm lasers with 505 nm long-pass filter and band-pass filters of 450/50, 530/30, and 660/20 nm. BD FACSDiva software was used for acquisition and data were analyzed using FlowJo. Samples were gated to exclude debris and cell doublets. The single-cell population was further gated for GFP staining. A stop gate of 10^4 cells was set on the GFP-positive gate. The percentage of cells containing an ASC speck was determined by analyzing the height (H), width (W), and area (A) of the GFP pulse area (high $H:A$ and low $W:A$ indicate speck-positive cells) as described previously by Sester and group (28, 29).

Inflammasome and Caspase-1 Activity Characterization and Evaluation

The protocol for ICCE is described in our previous study (24). Following inflammasome activation, media from each well was aspirated leaving 150 μ l and volume was made up to 200 μ l with media containing cell-permeable FLICA660-YVAD-FMK (FLICA660) (1:45 final dilution) (Immunochemistry Technologies; Cat. # 9122) and incubated for 30 min at 37°C with 5% CO₂. Cells were washed twice with 1 \times wash buffer (supplied with the FLICA kit). For ISXII acquisition, cells were treated with 50 μ l trypsin-EDTA (Corning; Cat. # 25-053-Cl) per well and fixed with 4% PFA (EMS; Cat. # 15710) for 15 min at room temperature. Following inflammasome activation and FLICA-600 treatment, THP-1 cells, immortalized wild-type and caspase-1/11^{-/-}, and primary human monocytes were fixed with 4% PFA for 15 min at room temperature, permeabilized with 0.1% Triton X-100 (Fisher Scientific; Cat. # BP151-100) for 10 min at room temperature and blocked in PBS containing 5% fish gelatin (Sigma Aldrich; Cat. # G7765), 1% BSA (Fisher Scientific; Cat. # BP1605-100), and 0.05% Triton X-100 for 1 h at room temperature. After blocking, cells were stained with rabbit anti-ASC (N15)-R (1:250) (Santa Cruz; Cat. # sc-22514-R) in wash buffer (PBS containing 1% fish gelatin, 1% BSA, and 0.5% Triton X-100) for 2 h. Cells were washed three times with wash buffer, followed by incubation with Alexa Fluor[®]488 goat-anti-rabbit IgG (1:500) (Life Technologies; Cat.# A11034) or Alexa Fluor[®]594 goat-anti-rabbit IgG_{2a} (1:1,000) (Life Technologies; Cat.# A21135) in wash buffer for 1 h. Fixed cells were harvested and stained with 1 μ g/ml DAPI (Invitrogen; Cat. # D-1306) in 1 \times PBS supplemented with 0.5 mM EDTA (cell suspension buffer) for 10 min at room temperature (RT). Cells were washed once with 1 \times PBS and resuspended in 50 μ l ISXII cell suspension buffer by gently tapping the tubes (use of a pipette or vortex mixer should be avoided at this stage). The samples were then acquired on the AMNIS ImageStream ISXII.

Colocalization

Colocalization of proteins with a resolution of 0.5 μ m per pixel in the X- and Y-axis can be determined with the AMNIS ISXII using Bright Detail Similarity (BDS index scores, a log-transformed Pearson's correlation coefficient) (30). A BDS index score ≥ 1.5 is considered significant for colocalization (31). The BDS index was calculated using the ASC speck mask

(mask 14) and FLICA spot mask (mask V) on a pixel-by-pixel and cell-by-cell basis with the Amnis IDEAS Colocalization Wizard tool. Using events from population S as an internal negative control, a threshold BDS index of 1.5 was set to determine colocalization of speck and active caspase-1 (FLICA) aggregates.

Microscopy

For microscopy, THP-1 cells were fixed and stained as described for ICCE. NLRP3 was stained using Cryopyrin (H-66) rabbit polyclonal IgG (1:1,000) (Santa Cruz; Cat. # sc-66846) or mouse monoclonal ANTI-FLAG[®] M2 antibody (1:1,000) (Sigma Aldrich; Cat. # F1804) while performing experiments in HEK293Ts. HEK293T cells were fixed with 4% PFA and washed three times with 1 \times PBS, dipped in distilled water, and mounted on a slide using 10 μ l of Fluoro-Gel II mounting medium with DAPI (EMS; Cat. # 17985-51) and visualized using an Axio Observer Z1 fluorescence microscope (Zeiss). Images were acquired using ZEN-Blue at an optimal setting to avoid saturation. Image acquisition was run at identical setting. Image analysis was performed using Fiji-ImageJ software. ASC-positive cells containing specks were counted manually from randomly selected fields acquired at $\times 20$ or $\times 60$ magnifications. The percentage of speck-containing cells was calculated as the fraction of ASC-positive cells containing specks. The percentage of cells containing GFP-RFP aggregates was calculated as the fraction of GFP-RFP-positive cells containing none, single, or multiple aggregates.

Quantification and Statistical Analysis

At least three independent experiments were performed with two/three technical repeats unless otherwise indicated. The statistical tests used for data analysis are stated in the figure legends. A p -value of ≤ 0.05 was considered statistically significant. All statistical analyses were performed using Prism 7.

RESULTS

Colchicine Prevents Speck Formation But Not Inflammasome Activation

Treatment of macrophages with nigericin concentrations above 3 μ M stimulates maturation and release of IL-1 β even in the presence of colchicine, a microtubule inhibitor that blocks speck assembly (32). Therefore, we considered that higher concentrations of nigericin might activate the inflammasome in the absence of the speck, but whether colchicine blockade of NLRP3:ASC speck assembly is overcome under these conditions is untested. PMA-treated THP-1 macrophages were stimulated with increasing concentrations of nigericin in the presence or absence of colchicine. In the absence of colchicine, nigericin stimulation led to maximal IL-1 β processing (~ 30 -fold over untreated controls) irrespective of the dose of nigericin (Figure 1A). At lower concentrations of nigericin (1 and 2.5 μ M), IL-1 β maturation and release was nearly blocked by colchicine treatment, but at 5 μ M, nigericin overcame this

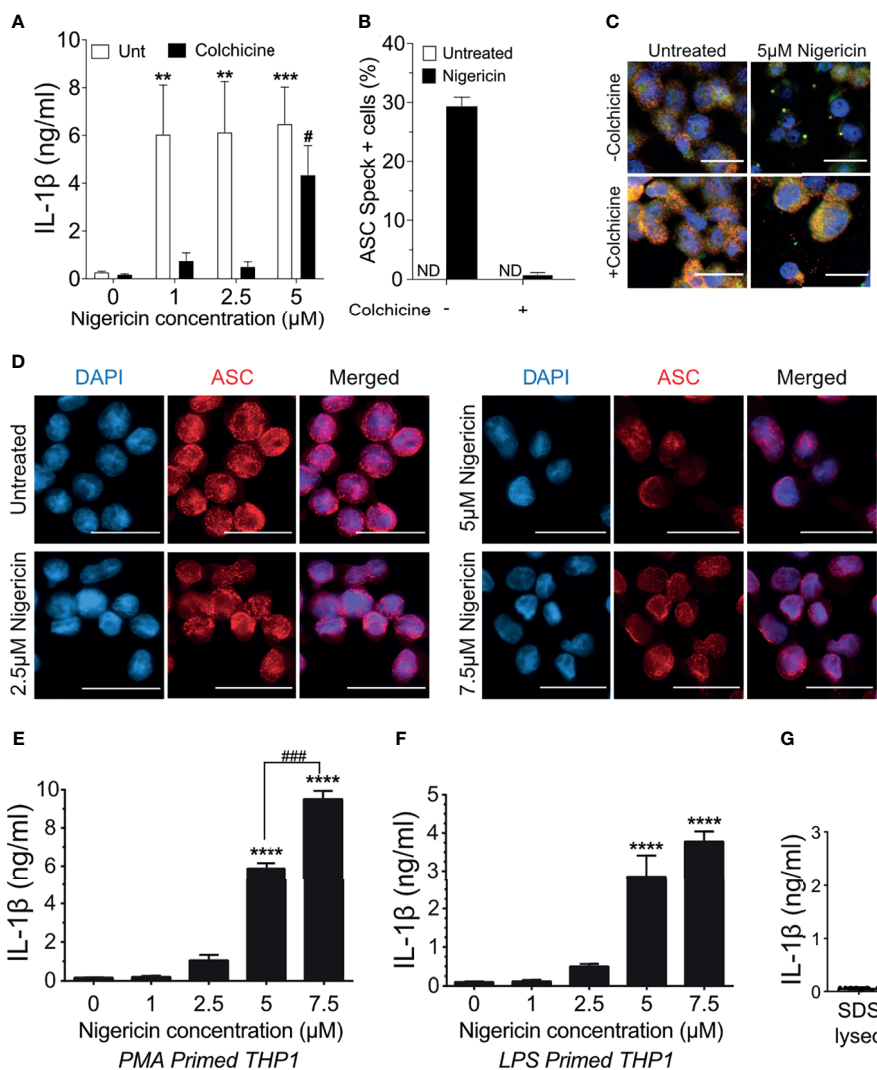


FIGURE 1 | Higher doses of nigericin induce IL-1 β release in the absence of specks. **(A)** THP-1 cells were treated with 100 nM phorbol 12-myristate 13-acetate (PMA) for 72 h and treated with 5 μ M colchicine for 1 h followed by stimulation with different doses of nigericin for 2 h. Culture supernatant was used for IL-1 β ELISA. **(B)** THP-1 cells were treated as described in **(A)**. Following nigericin stimulation, cells were fixed and stained for NLRP3 and ASC and analyzed for specks by microscopy. A minimum of 600 cells were analyzed per condition and counted for the presence of speck manually. Data represented as mean \pm SEM for two independent experiments. N.D., not detected. **(C)** Representative micrographs for data shown in **(B)**. Cells were stained for NLRP3 (red), ASC (green), and DAPI (blue). Scale bar = 25 nm. Single channel staining shown in **Figure S3**. **(D)** THP-1 cells were primed with 100 nM PMA for 72 h and treated with 5 μ M colchicine for 1 h followed by stimulation with nigericin at the indicated concentrations for 2 h. Cells were stained for ASC (red) and DAPI (blue). Scale bar = 25 nm. Representative micrographs are shown. **(E)** THP-1 cells were primed with 100 nM PMA for 72 h and treated with 5 μ M colchicine for 1 h followed by stimulation with nigericin at the indicated concentrations for 2 h. Culture supernatant was used for IL-1 β ELISA. **(F)** THP-1 cells were treated with 100 ng/ml of LPS for 3–4 h and treated with 5 μ M colchicine for 1 h followed by stimulation with nigericin at the indicated concentrations for 2 h. Culture supernatant was used for IL-1 β ELISA. **(G)** THP-1 cells were stimulated with PMA as in **(E)** and lysed with 0.09% Triton X-100. IL-1 β lysates were diluted 1:5 in assay buffer and measured by ELISA. Data represented as mean \pm SEM for a minimum of three independent experiments, unless otherwise mentioned. ** p < 0.01, *** p < 0.001, **** p < 0.0001 for comparison with respective untreated controls; two-way ANOVA followed by Dunnett's **(A)** multiple comparison tests. # p < 0.05, ### p < 0.001 Student's t -test for comparison between colchicine-treated cells stimulated with or without 5 μ M nigericin.

blockade (**Figure 1A**). Although somewhat reduced, the IL-1 β response to 5 μ M nigericin in the presence of colchicine was approximately 20-fold higher than the untreated control and 65% of that was seen without colchicine. While speck formation was expected to accompany inflammasome activity, less than 1% of colchicine-treated cells had ASC specks despite stimulation

with 5 μ M nigericin (**Figures 1B, C**). Thus, IL-1 β processing can occur in the absence of specks, and speck formation may not be essential for the NLRP3 inflammasome response.

Prevailing dogma equates speck assembly and inflammasome activation of caspase-1. However, increased speck frequency does not correlate well with the levels of released IL-1 β . For example,

PMA-treated THP-1 macrophages stimulated with 5 μM nigericin yielded approximately three-fold more speck-containing cells than those stimulated with 1 μM despite comparable IL-1 β release (data not shown). This lack of correlation between specks and the magnitude of the IL-1 β response together with the near complete blockade of IL-1 β when colchicine is used with lower doses of nigericin suggests the possibility that ASC specks might improve, or even maximize, caspase-1 activation by suboptimal stimuli. If correct, the IL-1 β response to nigericin is expected to be dose-dependent in the absence of specks. PMA-treated THP-1 macrophages were stimulated with colchicine and stimulated with increasing concentrations of nigericin (1.0 to 7.5 μM). In the presence of colchicine, specks were not observed in cells treated with any concentration of nigericin (**Figure 1D**) and little IL-1 β was produced after stimulation with up to 2.5 μM nigericin (**Figure 1E**). Interestingly, in the absence of specks (i.e., with colchicine), supernatant IL-1 β levels were dependent upon the dose of nigericin for concentrations between 2.5 and 7.5 μM . A similar dose dependency was observed with LPS-primed THP-1 (**Figure 1F**). In the presence of colchicine, higher concentrations of ATP and MSU were not evaluated because they induced cell death. We confirmed that the IL-1 β ELISA kit used does not detect uncleaved pro-IL-1 β (**Figure 1G**) released upon cell death. Thus, only IL-1 β actively cleaved following stimulation is detected in these assays. While these data demonstrate that the speck is not required for caspase-1 cleavage of IL-1 β , they do not rule out the ASC speck as a site of caspase-1 activity. Furthermore, these data also suggest that ASC specks facilitate and maximize caspase-1 cleavage of IL-1 β , perhaps through lowering the agonist threshold required for NLRP3 inflammasome activation.

Caspase-1 Activity Is Distal to the ASC Speck Organization Site

As IL-1 β processing can occur in the absence of ASC specks, the site of caspase-1 activation may be distinct from the speck structure when one is present. We previously demonstrated that ASC specks and caspase-1 activity can be visualized simultaneously in cells using imaging flow cytometry (24). Although our focus was on cells with specks and organized caspase-1 activity, we observed that active caspase-1 was distributed throughout the cytoplasm. We manually re-evaluated micrographs from these experiments to consider cells with individual specks and active caspase-1 regardless of organization. Inflammasome-reconstituted cells receiving either 20 or 50 ng of caspase-1 can be divided into four subpopulations based on their distribution of specks and active caspase-1 (**Figure 2A**): first, specks with coincident sites of active caspase-1 [concomitant speck and FLICA (C); 13.5%–21.2%]; second, specks and non-coincident (distant) discrete sites of active caspase-1 [separate speck and FLICA (S); 9.3%–9.6%]; third, diffuse caspase-1 activity that overlaps specks [diffuse FLICA (D); 66.1%–66.5%]; and fourth, diffuse caspase-1 activity distributed throughout the cells, but absent at the speck [non-FLICA specks (N); 24.8%–28%] (**Figures 2B, C**).

Importantly, the amount of transfected caspase-1 did not significantly alter these distribution patterns or the frequency of cells exhibiting each pattern (**Figures 2B, C**). Approximately 15%–20% of the cells had features of more than one distribution pattern for speck and active caspase-1 and were quantified as overlapping sets (**Figures 2B, C**). Populations with ASC specks and organized caspase-1 (S and C) account for 22%–30% of the cells (**Figures 2B, C**). In population S (2% to 4%), caspase-1 activity was organized and located distally to the ASC speck, suggesting an unexpected spatial disconnect between active caspase-1 and the speck in this subpopulation. Viewing a 3D event in 2D may cause two separate events in distinct planes to appear colocalized. To evaluate colocalization of ASC and active caspase-1 in cells with concomitant staining (population C) using the ImageStream, we used the BDS index function and IDEAS Colocalization Wizard Tool (see *Methods*). A BDS index of 3.0 indicates a high degree of colocalization (both objects are in the same focal plane), where an index of 1.0 is not colocalized (not in the same focal plane). Using events from population S as an internal negative control, the BDS index threshold was set to 1.5. The speck and active caspase-1 (FLICA) are considered colocalized in cells with scores ≥ 1.5 (**Figure 2D**). For nigericin-stimulated cells, the mean BDS index for the ASC speck and caspase-1 activity was approximately 0.25, irrespective of the amount of caspase-1 transfected (**Figure 2E**), indicating a lack of colocalization. Surprisingly, colocalization of the ASC speck and caspase-1 activity (BDS index ≥ 1.5) occurred in fewer than 2% of cells receiving 50 ng of caspase-1 and none of those receiving 20 ng (**Figure 2F**). Thus, even in population C, where specks and caspase-1 activity appear concomitant, ASC specks and the site of active caspase-1 are spatially separated. Indeed, approximately 90% of cells with specks had diffuse caspase-1 activity (populations D and N), and of these, roughly a third were devoid of caspase-1 activity at the speck itself (**Figures 2B, C**). Collectively, these data unexpectedly suggest that in cells with a discrete NLRP3:ASC speck, caspase-1 activity is almost exclusively separate from the speck structure.

Speck Formation Is Not Equivalent to IL-1 β Processing

Our analysis suggests that NLRP3:ASC speck and the inflammasome may be distinct entities. Alternatively, if the speck is the site of caspase-1 activity, speck formation should be proportional to IL-1 β production. While studies demonstrate that small molecule NLRP3 inhibitors or mutations in inflammasome components block both specks and IL-1 β maturation (18, 20, 33), we found no study reporting proportionality between speck frequency and IL-1 β maturation. NLRP3 contains a C8:C108 disulfide bond suggested to be important for NLRP3–ASC interaction (34). Individually, inflammasome activation does not strictly require cysteine 8 or 108, but IL-1 β production is increased by C108A and C108S single-point mutants and decreased by C8/108 double mutants (25, 35). Since ASC speck formation by these mutants is expected to reflect their inflammasome activity, we evaluated IL-1 β release and speck formation in inflammasome-reconstituted

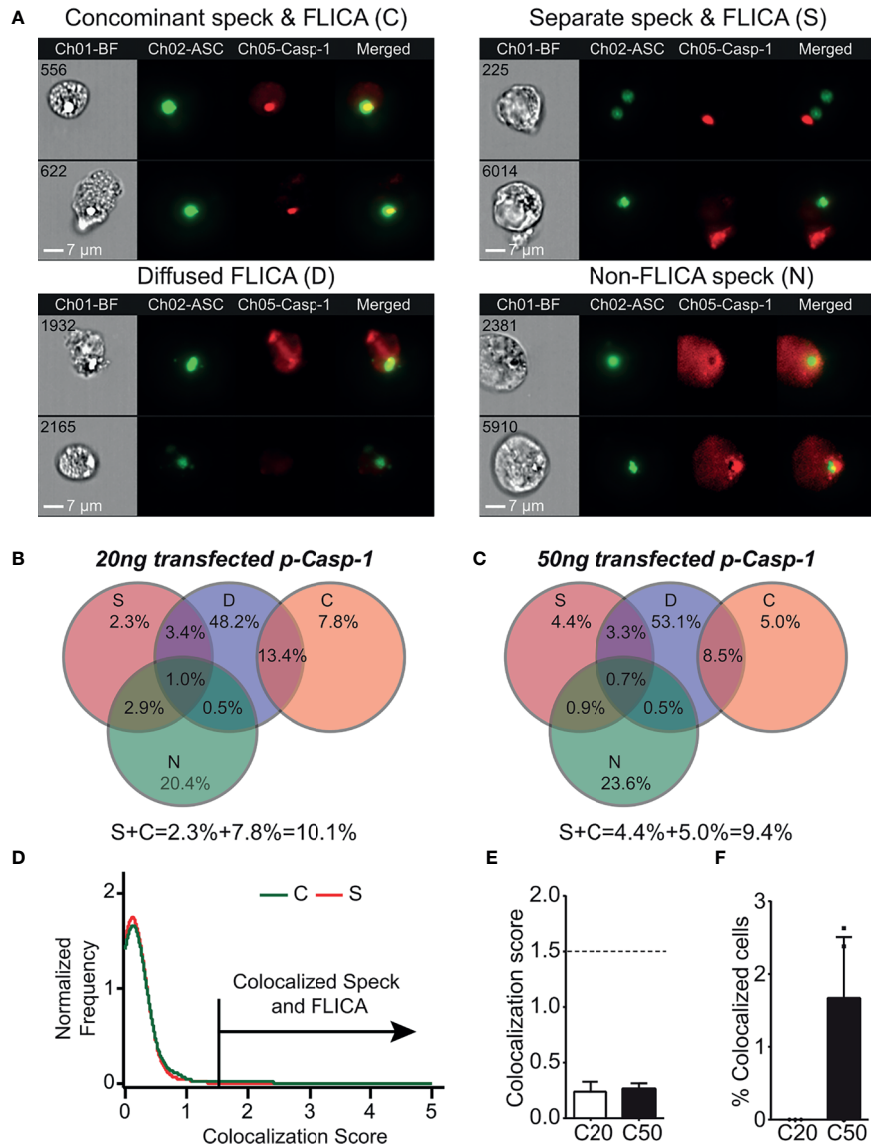


FIGURE 2 | Active caspase-1 does not colocalize with the ASC speck. HEK293T cells were transfected with 100 ng NLRP3, 50 ng GFP-ASC, and 20 or 50 ng CASP1 and treated with 5 μm nigericin for 2 h. ASC speck-positive cells were analyzed for distribution of active caspase-1 and ASC speck by inflammasome and caspase-1 activity characterization and evaluation (ICCE). Ch01-BF (brightfield), Ch02-GFP-ASC (green), Ch05-active caspase-1 (FLICA; red). The cells containing specks and active caspase-1 were manually segregated into four different subpopulations. **(A)** Representative images from the subpopulation of cells showing (top left) coincident ASC speck and active caspase-1 (**C**), (top right) distant ASC speck and active caspase-1 (**S**), (bottom left) diffused active caspase-1 (**D**), and (bottom right) specks lacking any detectable caspase-1 activity (**N**). The subpopulation of cells where active caspase-1 is diffused around the ASC speck. **(B)** Venn diagram showing the frequency of different subpopulations in cells transfected with 20 ng CASP1 (C20). **(C)** Venn diagram showing the frequency of different subpopulations in cells transfected with 50 ng CASP1 (C50). **(D)** Colocalization analysis of ASC speck and active caspase-1 of images shown in **(A)** (subpopulation C); histogram showing the threshold criteria for colocalization assay. **(E)** Mean colocalization score of images shown in **(A)**; a threshold score of 1.5 was selected as positive for colocalization. **(F)** Frequency of colocalized events over total events noted above the threshold line for C20 (20 ng) and C50 (50 ng) amount of transfected CASP1. Data represented as mean ± SEM for a minimum of three independent experiments. Data represented as mean for **(B)**.

HEK293T cells expressing C8 and C108 single and double mutants stimulated with nigericin or infected with *F. novicida* (Fn) U112. For Fn U112 infection, cysteine mutations had little impact on NLRP3-dependent IL-1β maturation or the frequency of ASC speck-containing cells (**Figure 3A**). However, with nigericin stimulation, IL-1β production increased approximately 1.5× for

single-point C108 mutants and decreased by 2× for C8/C108 double mutants relative to wtNLRP3, while speck frequency was diminished by approximately 25% for all C8 and C108 mutants (**Figure 3B**). Thus, IL-1β production by C8/C108 mutants correlated closely with ASC speck formation (IL-1β: speck ratio of about 1) in response to Fn U112 infection (**Figure 3C**), but was not correlated

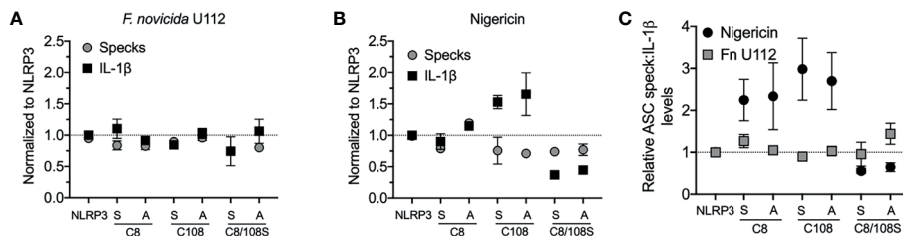


FIGURE 3 | N-terminal cysteine mutations uncouple speck formation and inflammasome function. (For ASC speck analysis) HEK293T cells were transfected with 50 ng of GFP-ASC with 100 ng NLRP3 or pcDNA3. Eighteen hours post-transfection, cells were either stimulated with nigericin agonists or left untreated, or 4 h after transfection, cells were infected with *Francisella novicida* (*Fn*). Cells were fixed at 2 h after stimulation (nigericin) or 24 h post-*Fn* infection and analyzed for ASC specks by time-of-flight inflammasome evaluation (TOFIE). (For IL-1 β release) HEK293T cells were transfected with 8 ng of myc-ASC with 100 ng NLRP3 or pcDNA3, 40 ng CASP1, and 200 ng IL1B. Eighteen hours post-transfection, cells were either stimulated with indicated agonists or left untreated. **(A)** Normalized ASC speck frequency (TOFIE) in comparison with normalized IL-1 β release in reconstituted 293T cells following *Fn* U112 infection. **(B)** Normalized ASC speck frequency (TOFIE) in comparison with normalized IL-1 β release in reconstituted 293T cells following nigericin stimulation. **(C)** Comparison of the ratio of normalized ASC specks frequency (TOFIE) with normalized IL-1 β release following NLRP3 activation by nigericin stimulation and *Fn* U112 infection.

when nigericin was used. Indeed, despite all C8/108 mutants having uniformly diminished speck frequency, single-point C8 mutants decreased nigericin-induced speck formation but had little impact on IL-1 β , where C108 mutants increased IL-1 β production despite diminished speck-forming capacity. C8/108 double mutants markedly decreased IL-1 β but had little further impact on nigericin-induced ASC speck formation. Thus, speck frequencies do not simply parallel or equate to inflammasome activity (IL-1 β production). That IL-1 β processing can increase or decrease irrespective of ASC speck formation is consistent with our hypothesis that the site of inflammasome IL-1 β processing is distinct from the ASC speck structure.

Our results with NLRP3 mutants provide compelling evidence that speck formation and inflammasome function are likely disconnected. Although speck formation follows stimulation with inflammasome agonists and precedes IL-1 β elaboration, they may not be the site of IL-1 β processing. If correct, other indications may be evident during agonist stimulation of wild-type NLRP3. Reconstitution of agonist-responsive NLRP3 inflammasomes is accomplished by transfecting limited quantities of inflammasome components encoding plasmids (36). In such experiments, ASC specks are rarely observed beyond background levels despite robust IL-1 β production comparable to similarly stimulated macrophages (data not shown). Indeed, to evaluate agonist-dependent induction of specks similar to that seen in macrophages, higher expression of NLRP3 and ASC is required (24, 28, 36). Therefore, we compared ASC speck formation capacity (TOFIE) and IL-1 β processing (inflammasome reconstitution assay) in HEK293Ts in response to agonists thought to use different activation pathways including pore formation/K⁺ efflux (nigericin), phagosome rupture (*Fn* infection and MSU stimulation), and ROS generation (H₂O₂). In cells expressing NLRP3, nigericin treatment induced a 15-fold increase in IL-1 β processing and an approximately three-fold increase in speck formation (Figure 4A). As expected, no significant speck formation or IL-1 β production occurred in unstimulated cells or those lacking NLRP3. Thus, speck formation and IL-1 β processing are positively correlated for

nigericin stimulation. However, *Fn* infection induced speck formation in the absence of NLRP3, but no IL-1 β processing above background was observed (Figure 4B). This result is consistent with a previous work reporting that specks form in the absence of NLRP3 but lack caspase-1 activity (37). In cells expressing NLRP3, *Fn* infection induced a robust IL-1 β release without a significant further increase in speck frequency (Figure 4B). Thus, for *Fn* infection, IL-1 β production (inflammasome function) appears disconnected from speck formation. *Fn*-induced inflammasome function, but not speck formation, is dependent on NLRP3. Surprisingly, neither H₂O₂ nor MSU induced speck formation, but significant levels of IL-1 β were produced (Figures 4C, D). In these experiments, approximately 25% of the cells contained a speck, but no IL-1 β was produced above controls without stimulation (Figures 4C, D). For H₂O₂ and MSU, speck formation does not equate directly with NLRP3 inflammasome activation. Thus, in inflammasome-reconstituted cells, agonists like H₂O₂ and MSU may activate the NLRP3 inflammasome without inducing specks.

As our H₂O₂ and MSU results were surprising, we considered that specks induced by these agonists may have been formed but rapidly degraded prior to enumeration. To evaluate this alternate hypothesis, speck formation was tracked for 60 min using increasing concentrations of H₂O₂ or MSU in cells expressing NLRP3 and ASC. H₂O₂ induces IL-1 β approximately 60 min after stimulation (Figure 4E). As expected, speck formation increased over time and with escalating nigericin stimulation (Figure 4F). Interestingly, no concentration of H₂O₂ tested induced speck formation above basal levels within 60 min, and no decrease in basal speck frequency was evident (Figure 4F). Results with MSU stimulation were essentially identical (Figure 4G). Consistent with the transfected cell data, neither H₂O₂ nor MSU induced specks in THP-1 cells (Supplementary Figure S4). Thus, rapid speck formation followed by degradation does not account for the absence of specks following H₂O₂ or MSU stimulation. Collectively, these data suggest that even when wild-type NLRP3 is considered, speck formation is not equivalent to IL-1 β processing, and thus, the inflammasome may be distinct from the speck.

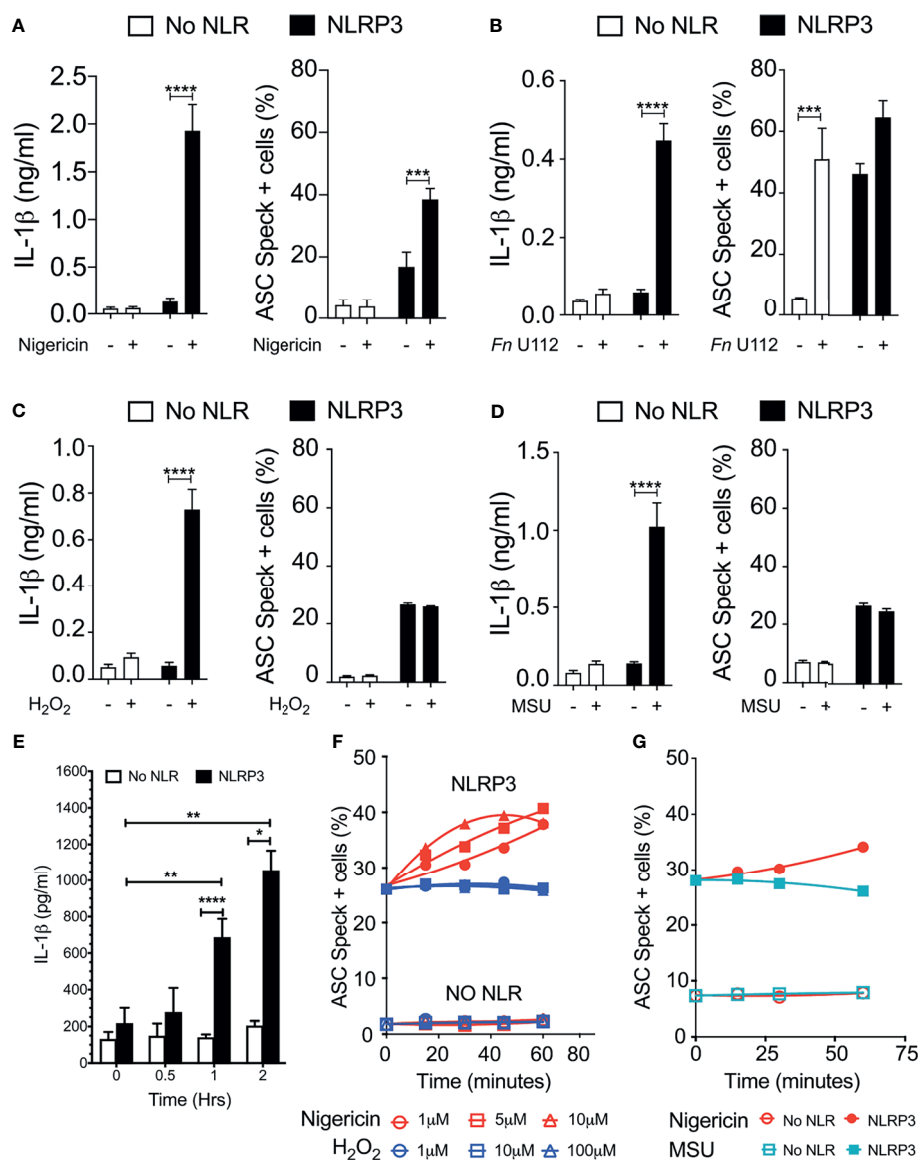


FIGURE 4 | Monosodium urate (MSU) and H₂O₂ elicit IL-1β without inducing ASC speck formation. Cells were transfected and stimulated for NLRP3 activation as described in the *Methods: Inflammasome Activation*. **(A)** IL-1β processing and speck formation exhibits positive correlation in nigericin-stimulated cells. **(B)** Unlike speck formation, IL-1β processing is dependent on NLRP3 in *F. novicida* U112-infected cells. **(C)** IL-1β and speck formation shows no correlation in H₂O₂-treated cells. H₂O₂-treated cells do not induce speck formation. **(D)** IL-1β and speck formation shows no correlation in MSU-treated cells. MSU-treated cells do not induce speck formation. **(E)** Time-course analysis of H₂O₂-treated IL-1β processing in inflammasome-reconstituted HEK293T cells. **(F)** Cells were treated with 5 μM nigericin (red) or 100 μM H₂O₂ (blue) for 1 h and analyzed for ASC speck+ cells by TOFIE. **(G)** Cells were treated with either 5 μM nigericin (red) or 150 μg/ml MSU (cyan) for 1 h and analyzed for ASC speck+ cells by TOFIE. Data represented as mean ± SEM for a minimum of three independent experiments **(A-E)**. Data represented as mean ± SEM for two independent experiments **(F, G)**. **p* < 0.05, ***p* < 0.01, ****p* < 0.001, *****p* < 0.0001 for comparison with respective untreated; two-way ANOVA followed by Sidak's multiple comparison tests.

Specks Are Dynamic and Negatively Correlated With IL-1β Release

Our data above strongly suggest that the speck is not necessary for inflammasome activity and that specks may function to instead facilitate inflammasome formation. As active caspase-1 is not localized to the speck, it follows that inflammasome complexes might form outside the speck or alternately be shed from the speck

upon caspase-1 activation. Since both the speck and the inflammasome require NLRP3:ASC interaction, envisioning how to demonstrate the formation of inflammasome structures outside the speck or shedding of such complexes is problematic. If inflammasomes form exclusively outside the speck, the speck is expected to be a static structure. In contrast, if the speck is shedding inflammasomes, its structure should be dynamic (e.g., size may be

altered with time and/or activation). To evaluate changes in ASC speck size during NLRP3 activation, we measured speck area in nigericin-stimulated cells expressing GFP-ASC, FLAG-NLRP3, and caspase-1 using our imaging flow cytometry-based ICCE assay (24). Both nigericin treatment and increasing the amount of available caspase-1 significantly decreased speck area (Figure 5A). The frequency of ASC speck-containing cells also decreased with increased caspase-1 expression in the absence of stimulation (Figure 5B). These inverse relationships demonstrate that caspase-1 activity negatively regulates both speck area and

speck formation and strongly suggest that ASC specks are dynamic in nature.

Since caspase-1 activity was negatively correlated with speck frequency in transfected cells, we also examined this relationship in macrophages. Nigericin was selected because neither H₂O₂ nor MSU induced specks in THP-1 cells (Supplementary Figure S4), and nigericin-induced speck formation appears to be directly correlated with IL-1 β processing (Figure 4A). No significant LDH release was detected over a 6-h time course (Figure 5C). PMA-primed THP-1 cells were activated with nigericin, and speck

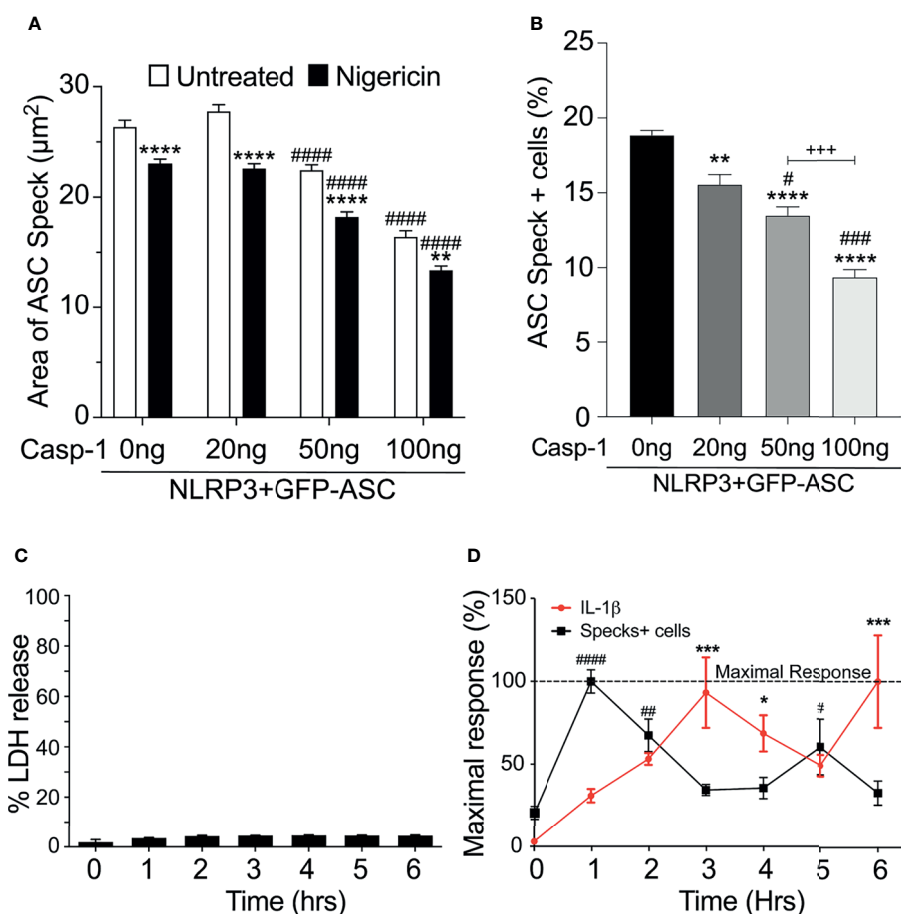


FIGURE 5 | Speck formation and IL-1 β release are cyclic and negatively correlated. **(A, B)** HEK293T cells were transfected with 50 ng GFP-ASC, 100 ng NLRP3, and 20 or 50 or 100 ng CASP1 and treated with 5 μ M nigericin for 2 h. Following nigericin treatment, cells were stained with FLICA, fixed, and analyzed for the presence of speck and active caspase-1 by ICCE. **(C, D)** PMA differentiated THP-1 cells are either left untreated (0 h) or treated with 5 μ M nigericin for 6 h. Culture supernatant was harvested at the stated time intervals to measure IL-1 β by ELISA and the release of LDH. Cells were fixed and stained for ASC to detect specks. **(A)** Cells were analyzed for the presence of ASC speck and active caspase-1 (positive for FLICA staining) from the double-positive gates as analyzed by ICCE. The area of the speck mask was calculated by ICCE. Data represented as mean \pm SEM for a minimum of three independent experiments. ** p < 0.01, **** p < 0.0001 for comparison with respective untreated, two-way ANOVA followed by Sidak's multiple comparison tests. ##### p < 0.0001 for comparison with respective untreated, two-way ANOVA followed by Dunnett's multiple comparison tests. **(B)** Cells positive for GFP-ASC were analyzed for the presence of ASC specks by ICCE. Data represented as mean \pm SEM for a minimum of three independent experiments. ** p < 0.01, **** p < 0.0001 for comparison with 0 ng transfected casp-1; # p < 0.05, ### p < 0.001 for comparison with 50 ng transfected casp-1; +++ p < 0.001 for comparison between 50 and 100 ng transfected casp-1; one-way ANOVA followed by Tukey's multiple comparison tests. **(C)** Percentage LDH release compared with 0.09% Triton X-100-lysed cells. **(D)** Line graph showing the frequency of ASC speck+ cells (red) and the release of IL-1 β (black). Data are normalized to maximal response of speck frequency and released IL-1 β over the time course of the experiment. Data represented as mean \pm SEM for a minimum of three independent experiments. * p < 0.05, *** p < 0.001, for comparison of IL-1 β release with untreated control (0 h); # p < 0.05, ## p < 0.01, #### p < 0.0001 for comparison of speck frequency with untreated control (0 h); one-way ANOVA followed by Sidak's multiple comparison tests.

formation and IL-1 β release were followed for 6 h; beyond 6 h, cells begin to detach from the plate complicating the assessment of speck formation. Specks were induced by nigericin, but their frequency was cyclical over time (**Figure 5D**) and reached maximum around 1 h. Speck frequency declined to near basal levels over the next 2 h, increased to about 50% of the maximum by 5 h post-stimulation, and then again decreased. IL-1 β release was also cyclical. IL-1 β levels increased over time but did not reach a maximum until around 3 h. By 5 h, IL-1 β levels had declined to about 50% of the maximum before increasing to near maximum levels around 6 h. Importantly, ASC specks were not detected outside the cells (data not shown). While both speck formation (frequency) and IL-1 β were cyclic in nature, they were out of phase, with IL-1 β increasing after peaks of speck formation. Although specks precede IL-1 β production, consistent with specks facilitating the production of IL-1 β , the temporal lag between speck frequency and IL-1 β levels (2 h for the first cycle) reveals that peak caspase-1 activity likely follows well after peak speck formation (see *Discussion*). Under *in vitro* conditions, the Vmax of caspase-1 in an NLR complex is around 2 nM/min (21). At this rate, the quantity of IL-1 β present at 3 h (5 ng/ml; ~0.3 nM) should have been converted in less than 1 min, i.e., with no temporal lag. Thus, it is likely that IL-1 β processing does not occur simultaneously with the formation of the speck, but instead develops gradually over time following speck formation.

Small Inflammasome Complexes Are Shed From the Speck

The physical and temporal separation of caspase-1 activity from specks suggests that inactive NLRP3:ASC:caspase-1 complexes might be shed from the speck with activation of caspase-1 and processing of IL-1 β occurring sometime later. If correct, cells with multiple sites of caspase-1 activity (with or without some diffuse activity) are expected to be abundant. Therefore, we evaluated the frequency of such cells in our HEK293T data from **Figure 2**. Nigericin-stimulated primary human macrophages and immortalized BMDMs were also examined. Multiple FLICA-stained sites indicating caspase-1 activity were observed in approximately 30% of speck-containing reconstituted HEK293T cells (**Figure 6A**), 55%–60% of speck-containing primary human macrophages stimulated with nigericin or ATP (**Figure 6B**), and 40% of nigericin-stimulated immortalized BMDMs (**Figure 6C**). While not direct evidence, the substantial number of cells with the expected phenotype is consistent with the shedding of inflammasome complexes from the speck. Speck-independent activation of small inflammasome complexes could also explain the observed pattern of caspase-1 activity. Indeed, small “death complexes” have been implicated in pyroptosis (caspase-1-dependent cell death) and IL-1 β processing after Aim2 and NLRC4 inflammasome activation in macrophages (33, 38).

To better distinguish between these possibilities, we attempted to address whether caspase-1 is activated in the vicinity of the speck or at some distance using various caspase-1 mutants (**Supplementary Figure S2A**). Cleaved caspase-1 p35/p10 is the active form and remains complexed with NLRP3:ASC until further cleavage generates inactive p10/p20 tetramers which leave the complex (39). Mutation of caspase-1 aspartic acids (D) 103 and 119 to asparagine (N) in caspase-1 UKN12 prevents

inactivating cleavage events and the dissociation of active caspase-1 (p35/p10) from the NLRP3:ASC complex. UKN1234 has mutations (D→N) in all four aspartic acid cleavage sites preventing its activation. Mutation of caspase-1 cysteine 285 to alanine alters the active site reducing activity (DEAD). Although FLICA staining appears to be caspase-1 specific (**Figure 6C**), others have suggested that FLICA reagents are promiscuous (40). Thus, for these experiments, the FRET-reporter GFP-YVAD-RFP was used to detect active caspase-1 (see *Methods*; **Supplementary Figure S1**). Wild-type and mutant caspase-1 activity measured using the GFP-YVAD-RFP reporter was comparable to that reflected by secreted IL-1 β levels, suggesting similar kinetics and specificity for both methods (**Supplementary Figures S2B, C**). Localization of GFP-RFP signal to a single perinuclear complex is expected if caspase-1 activation is occurring at the ASC speck. In contrast, multiple GFP-RFP aggregates would indicate that caspase-1 is activated outside the speck (**Figure 6D**). Active inflammasomes were reconstituted in HEK293T cells expressing wild-type or mutant caspase-1 in the presence of the GFP-YVAD-RFP reporter and evaluated for their GFP-RFP staining pattern by wide-field microscopy (single, multiple, or diffuse) (**Figure 6D**). No aggregates were observed in cells transfected with GFP-alone, RFP-alone, GFP with RFP, or the GFP-YVAD-RFP reporter (**Figures 6E, F**), indicating that these constructs do not spontaneously aggregate. With wild-type caspase-1, multiple GFP-YVAD-RFP complexes were present in 25% of the cells, while 50% had a single complex, and 25% had diffuse staining (**Figures 6D–G**). Using the activatable, non-released caspase-1 mutant UKN12 did not alter these frequencies. Both types of complexes were absent when caspase-1 was inhibited with a caspase-1-specific inhibitor (YVAD) or a pan-caspase inhibitor (ZVAD) and when the enzymatically inactive caspase-1 DEAD or uncleavable caspase-1 mutant UKN1234 was used. Some caspase-1-transfected cells had a single speck-like GFP-RFP aggregate (**Supplementary Figure S5A**). The absence of active caspase-1 colocalization with specks (**Figures 2E, F**) suggests this activity is near, but not coincident with, the ASC speck. In cells expressing the activatable, non-released UKN12 mutant, a zone of no GFP-RFP staining was observed at the likely position of the speck (**Supplementary Figure S5B**). This result is similar to that seen in the non-FLICA speck (N) cell population (**Figure 2A**). That UKN12 appears inactive at the likely position of the speck suggests that caspase-1 is activated after leaving the speck structure, not at the speck itself. Taken together, our data suggest that caspase-1 is most likely activated within small inflammasome complexes sometime after leaving the speck.

DISCUSSION

Caspase-1 Is Activated Outside the Speck

Our data provide the first clear demonstration that the speck is not the site of NLRP3-mediated caspase-1 activity. Instead, in both transfected cells and primary macrophages, NLRP3-activated caspase-1 is almost exclusively present in multiple

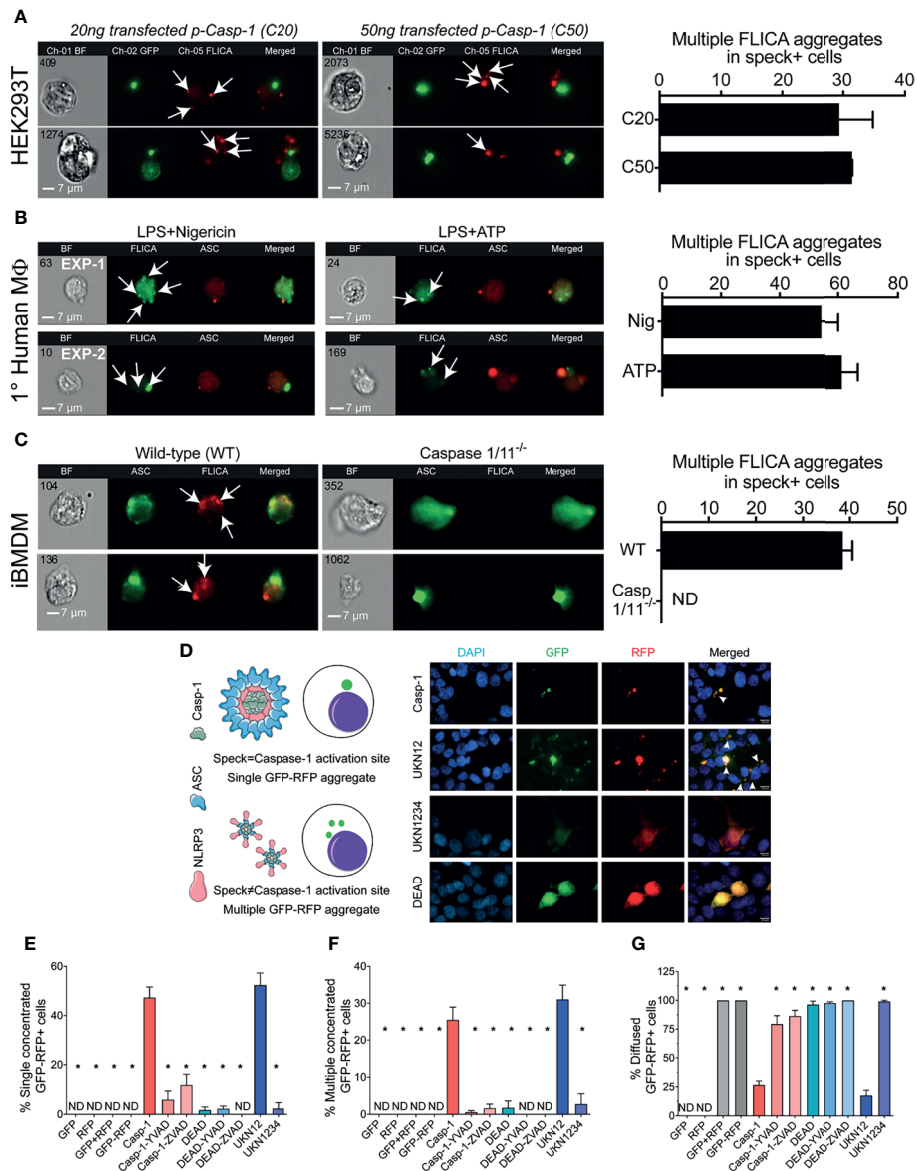


FIGURE 6 | NLRP3-dependent caspase-1 activity occurs at multiple cellular sites. LPS-primed primary human monocytes and immortalized BMDM cells were either left untreated or stimulated with 5 mM ATP or 10 μM nigericin for 30 min, stained with FLICA, and were fixed and analyzed by ICCE. HEK293T cells were transfected with 50 ng GFP-ASC with or without 100 ng NLRP3 and stimulated with 5 μM nigericin. Following nigericin stimulation, cells were stained with FLICA, fixed, and analyzed by ICCE. **(A)** (Left) The ASC (green) speck+ cells containing active caspase-1 (red) showed multiple FLICA (active caspase-1) aggregates in both cells transfected with 20 and 50 ng of CASP1. (Right) The frequency of cells containing speck and multiple FLICA aggregates. Data represented as mean ± SEM. **(B)** (Left) Primary human macrophages containing ASC speck (red) showing FLICA staining for active caspase-1 (green) as diffused and/or aggregated (multiple and distant from the speck). Representative images from two independent experiments are shown. (Right) The frequency of speck+ cells containing multiple FLICA aggregates. Data represented as mean ± SEM. **(C)** (Left) Immortalized BMDMs containing ASC speck (green) showing FLICA staining for active caspase-1 (red) as diffused and/or distant aggregates from ASC speck. Caspase-1/11^{-/-} BMDMs show no FLICA staining showing specificity of staining. (Right) The frequency of cells containing speck and multiple FLICA aggregates. Data represented as mean ± SEM. **(D–G)** HEK293T cells were transfected with 100 ng myc-ASC, 100 ng NLRP3, 400 ng CASP1 (WT or mutant), and 400 ng GFP-YVAD-RFP. Eighteen hours post-transfection, cells were fixed and analyzed for GFP-RFP aggregates by microscopy. **(D)** Schematic diagram showing expected outcomes with bifluorescent reporter if single/multiple sites of active caspase-1 are present. Representative micrographs showing distribution of active caspase-1 sites in a cell; DAPI (blue), GFP (green), RFP (red), and merged. White arrows show cells with multiple GFP-RFP aggregates. **(E)** Frequency of cells containing single concentrated GFP-RFP aggregates. **(F)** Frequency of cells containing multiple concentrated GFP-RFP aggregates. **(G)** Frequency of cells containing diffused GFP-RFP. Data represented as mean ± SEM for each field of view for at least three independent experiments. A minimum of 1,000 cells were analyzed for each condition. **p* < 0.0001, for comparison with casp-1-transfected sample, one-way ANOVA followed by Dunnett’s multiple comparison tests. ND, not detected.

cytoplasmic aggregates. This observation seemingly contradicts two studies suggesting that caspase-1 is activated at the NLRP3–ASC speck complex. In one, active caspase-1 was co-isolated with chemically crosslinked ASC (39). However, whether the caspase-1 activity observed in such studies was isolated from the speck itself or some other smaller complexes is uncertain as ASC crosslinking does not distinguish between these complexes. In the other study, active caspase-1 was colocalized to the center of the speck structure formed during NLRP3 inflammasome activation (41). Although we observed some cells with a similar coincident pattern, further analysis indicates vertical separation of the NLRP3:ASC speck and active caspase-1. In contrast to these studies, we observed that NLRP3 directed caspase-1 activity localized within multiple small cytoplasmic complexes. Consistent with our results, Akira et al. also observed multiple NLRP3–ASC complexes in IL-1 β -producing cells stimulated with monosodium urate crystals using proximity ligation assay (12), although the absence of a speck in these assays was not mentioned or discussed. Furthermore, we also observed this localization pattern with the caspase-1 mutant UKN12. As UKN12 cannot be released from the inflammasome complex upon activation (39), these data confirm the presence of multiple cytoplasmic inflammasome complexes distinct from the speck.

Speck Formation Is Not Essential or Sufficient for Inflammasome Response

Formation of the singular ASC speck is very rapid, occurring within 3 min of NLRP3 activation (7, 42). In addition, inhibiting speck assembly using small-molecule drugs (e.g., MCC950) or pyrin-related peptides (e.g., POP2) also impairs NLRP3 inflammasome activity (18, 43). Such observations have been interpreted to indicate that the speck is equivalent to the inflammasome or, at least, an initial step in inflammasome activation. However, despite this strong correlative evidence, no direct experimentation has confirmed that the speck is actually the inflammasome.

We previously noted that nigericin activates caspase-1 without discernable ASC speck formation in NLRP3 inflammasome-reconstituted HEK293T cells (24), leading us to question the requirement of specks for inflammasome function. In the present study, the sterile agonists MSU and H₂O₂ also induce IL-1 β processing without speck formation in HEK293T cells. Compan et al. observed that stimulation with 200 mg/ml of MSU for 16 h induced speck formation in BMDMs (37). In our hands, THP-1 cells only required 2 h of stimulation with 150 μ g/ml MSU to produce IL-1 β , and speck formation was absent (**Supplementary Figure S4**). Furthermore, the MSU used by Compan et al. was manufactured by a different company. Thus, these differences may account for the contrasting observations between the studies. Nevertheless, if MSU-induced specks form at 16 h in THP-1, this appears to be well after the initiation of IL-1 β processing. Of note, and as mentioned above, Akira et al. observed multiple NLRP3–ASC complexes, as opposed to single specks, upon stimulation with MSU (12). H₂O₂ induces inflammasome processing of IL-1 β in THP-1 and other cells (44), but no studies

report that H₂O₂ induced speck formation. In THP-1 cells, H₂O₂ did not stimulate speck formation (**Supplementary Figure S4**). Indeed, although inducing inflammasome activity, H₂O₂ may inhibit speck formation as suggested during *Streptococcus pneumoniae* infection (45).

Moreover, speck assembly does not necessitate activation of caspase-1. We observed that *Fn* U112 elicits ASC speck in cells lacking NLRP3, but IL-1 β processing is not detected. Others report that osmotic changes induce speck formation in the absence of NLRP3, but these cells also do not process IL-1 β (37). Moreover, chimeric NLRP3 constructs containing the pyrin domain of either NLRP1 or 2 form specks but not an active inflammasome (**Supplementary Figure S6**) (25). Of note, reconstitution of speck formation and inflammasome function requires different amounts of transfected ASC. When agonist-dependent inflammasome activation is reconstituted in HEK293T cells, specks are not evident; higher expression of ASC is required to observe agonist-dependent or independent speck formation (24), again supporting the conclusion that ASC speck formation and inflammasome function are distinct. Although surprising given the seemingly exclusive linkage between ASC specks and active inflammasomes, our data demonstrate that formation of an ASC speck is not required for NLRP3-dependent caspase-1 activation, nor is the ASC speck sufficient for caspase-1 activation.

The Speck Lowers the Agonist Threshold for NLRP3 Inflammasome Activation

If neither required for NLRP3 inflammasome activation nor sufficient, what is the function of the speck? Given the prion-like polymerization of ASC and caspase-1 along with the defined perinuclear localization of singular specks in cells, the ASC speck has been suggested to be a supramolecular organizing center (SMOC) (8–10). SMOCs are cell location-specific higher-order signaling complexes that concentrate signaling components to facilitate binary, all-or-none, responses through a cooperative assembly mechanism (8–10). An ASC SMOC is expected to recruit most if not all of the available ASC and caspase-1 to the structure, maximize proximity-induced activation of caspase-1, and reduce the threshold of activation. Thus, activation of caspase-1 in this fashion should also occur in an essentially binary, “on–off” fashion. Why caspase-1 is not obligately activated upon speck formation is puzzling, but our data offer some insight.

NLRP1 or NLRP2 pyrin domain chimeras of NLRP3 form specks (**Supplementary Figure S6A**) and *Fn* U112 elicits ASC specks in cells lacking NLRP3. Yet, IL-1 β processing is either absent or significantly reduced versus controls in both cases (**Supplementary Figure S6B**). The simplest interpretation is that a specific NLR is required to either recruit or activate recruited caspase-1. However, this conflicts with current paradigms. Oligomerization of ASC recruits caspase-1 (20), and once recruited, caspase-1 is expected to undergo proximity-induced activation (46). Paradoxically, our data indicate that NLRP3-dependent caspase-1 activity is found in small cytosolic complexes distinct from the speck. Furthermore, activity of the

caspace-1 UKN12 mutant (activatable, non-dissociating) was also not localized to the speck. As UKN12 cannot dissociate from NLRP3:ASC and UKN12, complexes with active UKN12 must have been activated either independently or after release from the speck (39). A potential resolution to this dilemma is that while small, non-speck NLRP3 inflammasome complexes can form without the speck itself, the speck facilitates the formation and release of small inflammasome complexes, thereby amplifying or lowering the threshold for inflammasome activation. Consistent with this idea, Dick et al. suggest that the NLRC4-induced ASC speck serves as a signal amplification mechanism through the formation of multiple caspace-1 activation sites (33). While exploration of this hypothesis is needed, the seminal studies of extracellular inflammasomes/specks do not appear to be contradictory (42, 47).

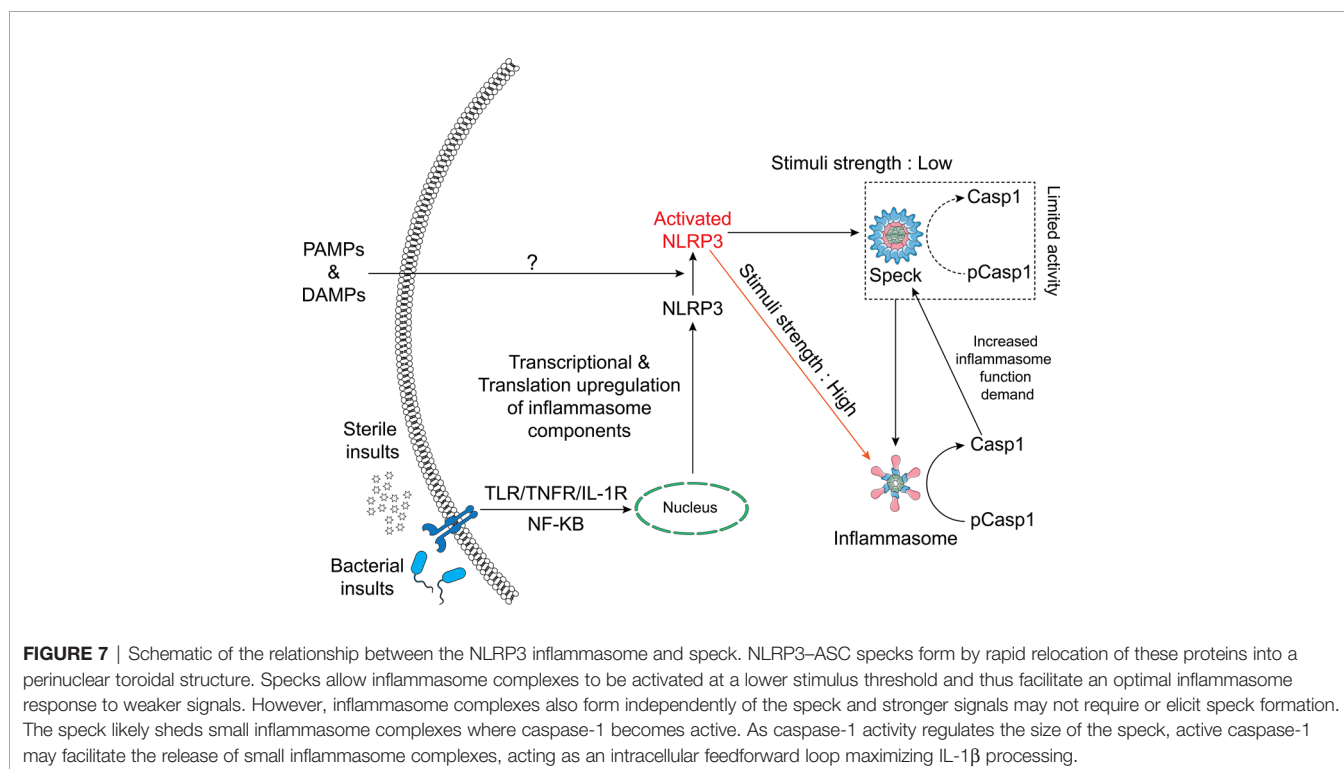
Such a mechanism might also help explain the threshold effect of the speck for nigericin-induced NLRP3 inflammasome activation. When speck formation is inhibited with colchicine, low-dose nigericin fails to activate the NLRP3 inflammasome, but higher doses of nigericin still elicit IL-1 β (32, 48). In our hands, higher doses of nigericin elicited IL-1 β maturation without speck assembly. Notably, when speck formation was inhibited by colchicine, nigericin induction of IL-1 β was largely dose dependent. In contrast, without colchicine, IL-1 β was elaborated at or near maximal levels irrespective of the nigericin concentration used. Thus, while not essential for NLRP3 inflammasome activation and unlikely the site of caspace-1 activity, the speck reduces the threshold required for agonist induction of full caspace-1 activity. Our findings are consistent with the NLRP3:ASC speck having

SMOC-like behavior lowering the threshold of inflammasome activation. However, the physical separation of caspace-1 activity from the ASC speck suggests that the NLRP3:ASC SMOC facilitates the formation and release of small, cytosolically active inflammasomes. Although consistent with our data, this hypothetical mechanism requires further investigation.

The Speck Is a Dynamic Structure Regulated by Caspace-1

Whether the ASC speck is a SMOC that facilitates the formation and release of small inflammasome complexes is unclear, and demonstrating this presents numerous challenges. ASC specks are larger in cells with enzymatically inactive caspace-1 (caspace-1 DEAD) compared with cells with wild-type caspace-1 (49). Moreover, ASC specks formed by ASC alone are larger than NLRP3:ASC specks, and the size of NLRP3:ASC specks is further reduced after nigericin stimulation (24). In this study, NLRP3:ASC speck size was inversely proportional to caspace-1 activity and nigericin stimulation further reduced the size of these specks. Thus, speck size is dynamic and is regulated by caspace-1 activity likely resulting from triggering of NLRP3. This change in size suggests that NLRP3 activation of caspace-1 may allow shedding of component proteins from the speck and could account for the presence of multiple cytosolic sites of inflammasome caspace-1 activity. While a change in protein conformation and/or spatial organization could account for the reduction in speck size, such changes do not help explain the multiplicity of active caspace-1 sites.

Interestingly, specks and inflammasome function are not only spatially separated but temporally distinct as well. We found that



speck frequency and IL-1 β processing were negatively correlated over time. Furthermore, the relationship between specks and IL-1 β processing was also cyclical with declines from peak speck frequency preceding IL-1 β processing, suggesting an inverse relationship between the speck and inflammasome function. Furthermore, in inflammasome-reconstituted HEK293T cells, abundant IL-1 β processing occurred in the relative absence of ASC specks, but prior to their peak (~7%) at 14 h (**Supplementary Figures S6C–F**). Curiously, osmotic stress-induced ASC specks in bone marrow-derived macrophages also suggest a similar inverse relationship between the speck and inflammasome activity (37). The temporal disconnect between speck formation and inflammasome function provides additional evidence that speck function is dynamic. Moreover, ASC speck formation might not be irreversible as believed.

In summary, we conclude that ASC specks and NLRP3 inflammasomes are distinct entities and that not all NLRP3 inflammasome agonists trigger speck formation. While small active NLRP3 inflammasome complexes are dispersed throughout the cell following activation and caspase-1 activity is not present at the NLRP3:ASC speck, the speck appears to enhance this process by reducing the threshold of stimulus needed for maximal caspase-1 activation. Our data suggest that when specks are formed, NLRP3 inflammasome IL-1 β processing and speck size are related in a dynamic and cyclical process regulated by caspase-1. We propose a refined hypothetical model for the relationship between the NLRP3 speck and inflammasome where the formation of an NLRP3:ASC: caspase-1 speck is energetically favored and releases small active inflammasome complexes but is not required to generate them (**Figure 7**).

DATA AVAILABILITY STATEMENT

The original contributions presented in the study are included in the article/**Supplementary Material**, further inquiries can be directed to the corresponding author.

AUTHOR CONTRIBUTIONS

Conceptualization, methodology, validation, and writing: AN and JH. Investigation, formal analysis, and visualization: AN and TR. Resources, supervision, and funding acquisition: JH. All authors contributed to the article and approved the submitted version.

FUNDING

This work was supported in part by NIH Grants R01AI072259, P01AI056320 (subproject 2), and R03AI146596 to JH.

ACKNOWLEDGMENTS

We thank Drs. Jim Drake and William O'Connor (Albany Medical College, Albany, NY) for their insightful comments on initial drafts

of the manuscript. Adobe Illustrator 2020 and Servier Medical Art templates have been used to draw the schematics.

SUPPLEMENTARY MATERIAL

The Supplementary Material for this article can be found online at: <https://www.frontiersin.org/articles/10.3389/fimmu.2021.752482/full#supplementary-material>

Supplementary Figure S1 | Schematic representation of FRET based bi-fluorescent caspase-1 activity reporter. **(A)** Schematic representation of bi-fluorescent reporter for caspase-1 activity. GFP and RFP are linked by the caspase-1-specific recognition amino acid sequence “YVAD”, which is also present in pro-IL-1 β . **(B)** The expected distribution patterns of caspase-1 reporter before, during, and after caspase-1 activation. **(C)** Schematic showing the cleavage states of the bi-fluorescent reporter allowing FRET-quantitation of cleavage by caspase-1.

Supplementary Figure S2 | Schematic representation of Caspase-1 mutants, their physiological phenotype and a FRET based bi-fluorescent caspase-1 activity reporter. HEK293T cells were transfected with 100 ng Flag-NLRP3, 100 ng myc-ASC, 400 ng IL1B (B) or GFP-YVAD (D), 400 ng CASP1 (WT or mutants) or empty vector (EV). **(A)** Schematic representation of caspase-1 mutants and their expected phenotypes. The position of five aspartic acid residues are shown (103, 119, 297, 314 and 315). Aspartic acids 103 and 119 are the cleavage sites between the CARD domain and p20 subunit of caspase-1. Aspartic acid residues 297 and 314/315 are the cleavage sites between the p20 and p10 subunit of caspase-1. The caspase-1 UKN12 mutant (D103N/D119N) can be activated but cannot be released or deactivated. All the aspartic acid cleavage sites have in the caspase-1 UKN1234 mutant have D→N mutations, making this mutant non-activatable. The caspase-1 DEAD mutant has the caspase deactivating C285A active site mutation. **(B)** The gating strategy to determine caspase-1 activation by flow cytometry. (From left to right: Top) The SSC-A vs FSC-A plot allows to eliminate debris and gate for cells. The FSC-W vs FSC-A plot allows to gate for single cells. The singlets were then plotted for optimum GFP intensity (PE-A vs FITC-A). The optimum GFP intensity cells were then plotted for FRET and a quadrant gate was made to determine FRET positive cells. Representative plots showing the absence of events in FRET channel for cells transfected with GFP-alone or GFP and RFP expressed on different plasmids. Events in FRET channel can be recorded only in cells transfected with GFP-YVAD-RFP. (Bottom) The quadrant plot showing FRET intensity of GFP-YVAD-RFP (bi-fluorescent reporter) in FRET channel of samples transfected with caspase-1 or caspase-1 DEAD. Bar graphs showing % FRET positive cells and % caspase-1 activity (Calculations in Methods and Materials) **(C)**. 24 hours post-transfection, culture supernatant was collected and IL-1 β was measured by ELISA

Supplementary Figure S4 | NLRP3 inflammasome activation does not necessitate ASC speck formation. **(A)** THP-1 cells were primed with LPS for 4 hours and stimulated with the stated agonist (See **Methods**) Cells were fixed and permeabilized. Cells were stained for ASC and nuclei were stained with DAPI. Cells were analyzed for presence of specks. Scale bar = 50 μ m. White arrows denote specks, yellow arrowhead indicates extracellular specks and red arrow indicates examples of non-speck cells. **(B)** Percentage of cells with intracellular specks and extracellular specks from A. Minimum of 100 cells from 3 field of views were analyzed. Mean percentages \pm SEM are shown; **p < 0.01 & *p < 0.5, for comparison with untreated sample, one-way ANOVA followed by Dunnett's multiple comparison tests.

Supplementary Figure S5 | Bi-fluorescent reporter recapitulates FLICA-like staining of active caspase-1. HEK293T cells were transfected with 100 ng myc-ASC, 100 ng NLRP3, 400 ng CASP1 (WT or UKN 12 mutant) and 400 ng GFP-YVAD-RFP. 18 hours post-transfection, cells were fixed, stained with DAPI and analyzed for GFP-RFP localization by microscopy. Colocalization (yellow) of GFP (green) and RFP (red) indicate binding of GFP-YVAD-RFP to active caspase-1 and thus reflects the cellular distribution of active caspase-1 sites. **(A)** (Top) Speck-like reporter fluorescence in some cells (red arrows; ~48% of cells,). (Bottom) Multiple reporter aggregates in some cells (white arrows; ~25% of cells,). **(B)** Two representative micrographs (top and

bottom) showing a reporter-free region close to nucleus (white arrow; expected site of the speck; observable only with diffuse staining). Images are representative of three independent experiments.

Supplementary Figure S6 | Uncoupling of speck formation and IL-1 β processing. **(A)** HEK293T cells were transfected with 1 μ g myc-ASC and 1 μ g Flag-NLRP3 or a chimeric Flag-NLRP133 or Flag-NLRP233. After 18 hours cells, fixed and permeabilized cells were stained with anti-Flag (M2) and anti-ASC (Santa Cruz) and then analyzed for speck formation. Percentage of cells containing specks. Minimum of 140 cells were counted from 4 individual field of view; for NLRP233, 30

cells were counted. Data is presented as Mean \pm SEM and analyzed using one-way ANOVA followed by Tukey's multiple comparison test. **(B)** IL-1 β processing in inflammasome reconstituted HEK293Ts expressing NLRP3 or the indicated chimeras and treated/infected with stated NLRP3 agonists (See **Methods**).

(C-F) HEK293T cells were transfected with 100 ng NLRP3, 100 ng GFP-ASC, 20 ng CASP1 and 200 ng IL1B allowing agonist-independent maturation and release of active IL-1 β . At stipulated time-points, cells and culture supernatants were harvested. Cells were fixed and analyzed for GFP expression **(C)**. Culture supernatant was analyzed for released IL-1 β **(D)**, ASC speck **(E)** and speck diameter **(F)**.

REFERENCES

- Latz E, Xiao TS, Stutz A. Activation and Regulation of the Inflammasomes. *Nat Rev Immunol* (2013) 13(6):397–411. doi: 10.1038/nri3452
- Cheng J, Waite AL, Tkaczyk ER, Ke K, Richards N, Hunt AJ, et al. Kinetic Properties of ASC Protein Aggregation in Epithelial Cells. *J Cell Physiol* (2010) 222(3):738–47. doi: 10.1002/jcp.22005
- Lamkanfi M, Dixit VM. Mechanisms and Functions of Inflammasomes. *Cell* (2014) 157(5):1013–22. doi: 10.1016/j.cell.2014.04.007
- Sharma D, Kanneganti TD. The Cell Biology of Inflammasomes: Mechanisms of Inflammasome Activation and Regulation. *J Cell Biol* (2016) 213(6):617–29. doi: 10.1083/jcb.201602089
- Shi J, Zhao Y, Wang K, Shi X, Wang Y, Huang H, et al. Cleavage of GSDMD by Inflammatory Caspases Determines Pyroptotic Cell Death. *Nature* (2015) 526(7575):660–5. doi: 10.1038/nature15514
- Hoss F, Rodriguez-Alcazar JF, Latz E. Assembly and Regulation of ASC Specks. *Cell Mol Life Sci* (2017) 74(7):1211–29. doi: 10.1007/s00018-016-2396-6
- Stutz A, Horvath GL, Monks BG, Latz E. ASC Speck Formation as a Readout for Inflammasome Activation. *Methods Mol Biol* (2013) 1040:91–101. doi: 10.1007/978-1-62703-523-1_8
- Kagan JC. Signaling Organelles of the Innate Immune System. *Cell* (2012) 151(6):1168–78. doi: 10.1016/j.cell.2012.11.011
- Kagan JC, Magupalli VG, Wu H. SMOCs: Supramolecular Organizing Centres That Control Innate Immunity. *Nat Rev Immunol* (2014) 14(12):821–6. doi: 10.1038/nri3757
- Wu H. Higher-Order Assemblies in a New Paradigm of Signal Transduction. *Cell* (2013) 153(2):287–92. doi: 10.1016/j.cell.2013.03.013
- Fernandes-Alnemri T, Wu J, Yu JW, Datta P, Miller B, Jankowski W, et al. The Pyroptosome: A Supramolecular Assembly of ASC Dimers Mediating Inflammatory Cell Death via Caspase-1 Activation. *Cell Death Differ* (2007) 14(9):1590–604. doi: 10.1038/sj.cdd.4402194
- Misawa T, Takahama M, Kozaki T, Lee H, Zou J, Saitoh T, et al. Microtubule-Driven Spatial Arrangement of Mitochondria Promotes Activation of the NLRP3 Inflammasome. *Nat Immunol* (2013) 14(5):454–60. doi: 10.1038/ni.2550
- Elliott EI, Sutterwala FS. Initiation and Perpetuation of NLRP3 Inflammasome Activation and Assembly. *Immunol Rev* (2015) 265(1):35–52. doi: 10.1111/imr.12286
- Li X, Thome S, Ma X, Amrute-Nayak M, Finigan A, Kitt L, et al. MARK4 Regulates NLRP3 Positioning and Inflammasome Activation Through a Microtubule-Dependent Mechanism. *Nat Commun* (2017) 8:15986. doi: 10.1038/ncomms15986
- Bryan NB, Dorfluetner A, Rojanasakul Y, Stehlik C. Activation of Inflammasomes Requires Intracellular Redistribution of the Apoptotic Speck-Like Protein Containing a Caspase Recruitment Domain. *J Immunol* (2009) 182(5):3173–82. doi: 10.4049/jimmunol.0802367
- Martinon F, Petrilli V, Mayor A, Tardivel A, Tschopp J. Gout-Associated Uric Acid Crystals Activate the NALP3 Inflammasome. *Nature* (2006) 440(7081):237–41. doi: 10.1038/nature04516
- Dalbeth N, Lauterio TJ, Wolfe HR. Mechanism of Action of Colchicine in the Treatment of Gout. *Clin Ther* (2014) 36(10):1465–79. doi: 10.1016/j.clinthera.2014.07.017
- Coll RC, Robertson AAB, Chae JJ, Higgins SC, Muñoz-Planillo R, Inserra MC, et al. A Small-Molecule Inhibitor of the NLRP3 Inflammasome for the Treatment of Inflammatory Diseases. *Nat Med* (2015) 21(3):248–55. doi: 10.1038/nm.3806
- Martinon F, Burns K, Tschopp J. The Inflammasome: A Molecular Platform Triggering Activation of Inflammatory Caspases and Processing of proIL-Beta. *Mol Cell* (2002) 10(2):417–26. doi: 10.1016/S1097-2765(02)00599-3
- Lu A, Magupalli VG, Ruan J, Yin Q, Atianand MK, Vos MR, et al. Unified Polymerization Mechanism for the Assembly of ASC-Dependent Inflammasomes. *Cell* (2014) 156(6):1193–206. doi: 10.1016/j.cell.2014.02.008
- Faustin B, Bartigue L, Bruey JM, Luciano F, Sergienko E, Bailly-Maitre B, et al. Reconstituted NALP1 Inflammasome Reveals Two-Step Mechanism of Caspase-1 Activation. *Mol Cell* (2007) 25(5):713–24. doi: 10.1016/j.molcel.2007.01.032
- Martinon F, Agostini L, Meylan E, Tschopp J. Identification of Bacterial Muramyl Dipeptide as Activator of the NALP3/cryopyrin Inflammasome. *Curr Biol* (2004) 14(21):1929–34. doi: 10.1016/j.cub.2004.10.027
- Atianand MK, Duffy EB, Shah A, Kar S, Malik M, Harton JA. Francisella Tularensis Reveals a Disparity Between Human and Mouse NLRP3 Inflammasome Activation. *J Biol Chem* (2011) 286(45):39033–42. doi: 10.1074/jbc.M111.244079
- Nagar A, DeMarco RA, Harton JA. Inflammasome and Caspase-1 Activity Characterization and Evaluation: An Imaging Flow Cytometer-Based Detection and Assessment of Inflammasome Specks and Caspase-1 Activation. *J Immunol* (2019) 202(3):1003–15. doi: 10.4049/jimmunol.1800973
- Rahman T, Nagar A, Duffy EB, Okuda K, Silverman N, Harton JA. NLRP3 Sensing of Diverse Inflammatory Stimuli Requires Distinct Structural Features. *Front Immunol* (2020) 11:1828. doi: 10.3389/fimmu.2020.01828
- Sherer NM, Lehmann MJ, Jimenez-Soto LF, Ingmundson A, Horner SM, Cicchetti G, et al. Visualization of Retroviral Replication in Living Cells Reveals Budding Into Multivesicular Bodies. *Traffic* (2003) 4(11):785–801. doi: 10.1034/j.1600-0854.2003.00135.x
- Thornberry NA, Bull HG, Calaycay JR, Chapman KT, Howard AD, Kostura MJ, et al. A Novel Heterodimeric Cysteine Protease Is Required for Interleukin-1 Beta Processing in Monocytes. *Nature* (1992) 356(6372):768–74. doi: 10.1038/356768a0
- Sester DP, Thygesen SJ, Sagulenko V, Vajjhala PR, Cridland JA, Vitak N, et al. A Novel Flow Cytometric Method to Assess Inflammasome Formation. *J Immunol* (2015) 194(1):455–62. doi: 10.4049/jimmunol.1401110
- Sester DP, Zamoshnikova A, Thygesen SJ, Vajjhala PR, Cridland SO, Schroder K, et al. Assessment of Inflammasome Formation by Flow Cytometry. *Curr Protoc Immunol* (2016) 114:14.40 1–14 40 29. doi: 10.1002/cpim.13
- Beum PV, Lindorfer MA, Hall BE, George TC, Frost K, Morrissey PJ, et al. Quantitative Analysis of Protein Co-Localization on B Cells Optimized With Rituximab and Complement Using the ImageStream Multispectral Imaging Flow Cytometer. *J Immunol Methods* (2006) 317(1-2):90–9. doi: 10.1016/j.jim.2006.09.012
- Wortzel I, Hanoch T, Porat Z, Hauser A, Seger R. Mitotic Golgi Translocation of ERK1c Is Mediated by a PI4KIIIbeta-14-3-3gamma Shuttle Complex. *J Cell Sci* (2015) 128(22):4083–95. doi: 10.1242/jcs.170910
- Gao W, Yang J, Liu W, Wang Y, Shao F. Site-Specific Phosphorylation and Microtubule Dynamics Control Pyrin Inflammasome Activation. *Proc Natl Acad Sci USA* (2016) 113(33):E4857–66. doi: 10.1073/pnas.1601700113
- Dick MS, Sborgi L, Rühl S, Hiller S, Broz P. ASC Filament Formation Serves as a Signal Amplification Mechanism for Inflammasomes. *Nat Commun* (2016) 7:11929. doi: 10.1038/ncomms11929
- Bae JY, Park HH. Crystal Structure of NALP3 Protein Pyrin Domain (PYD) and Its Implications in Inflammasome Assembly. *J Biol Chem* (2011) 286(45):39528–36. doi: 10.1074/jbc.M111.278812

35. Hafner-Bratkovic I, Sušjany P, Lainšček D, Tapia-Abellán A, Cerović K, Kadunc L, et al. NLRP3 Lacking the Leucine-Rich Repeat Domain Can be Fully Activated *via* the Canonical Inflammasome Pathway. *Nat Commun* (2018) 9(1):5182. doi: 10.1038/s41467-018-07573-4
36. Shi H, Murray A, Beutler B. Reconstruction of the Mouse Inflammasome System in HEK293T Cells. *Bio Protoc* (2016) 6(21):e1986. doi: 10.21769/BioProtoc.1986
37. Compan V, Martín-Sánchez F, Baroja-Mazo A, López-Castejón G, Gomez AI, Verkhatsky A, et al. Apoptosis-Associated Speck-Like Protein Containing a CARD Forms Specks But Does Not Activate Caspase-1 in the Absence of NLRP3 During Macrophage Swelling. *J Immunol* (2015) 194(3):1261–73. doi: 10.4049/jimmunol.1301676
38. Broz P, von Moltke J, Jones JW, Vance RE, Monack DM. Differential Requirement for Caspase-1 Autoproteolysis in Pathogen-Induced Cell Death and Cytokine Processing. *Cell Host Microbe* (2010) 8(6):471–83. doi: 10.1016/j.chom.2010.11.007
39. Boucher D, Monteleone M, Coll RC, Chen KW, Ross CM, Teo JL, et al. Caspase-1 Self-Cleavage Is an Intrinsic Mechanism to Terminate Inflammasome Activity. *J Exp Med* (2018) 215(3):827–40. doi: 10.1084/jem.20172222
40. Darzynkiewicz Z, Pozarowski P. All That Glitters Is Not Gold: All That FLICA Binds Is Not Caspase. A Caution in Data Interpretation—and New Opportunities. *Cytometry A* (2007) 71(8):536–7. doi: 10.1002/cyto.a.20425
41. Man SM, Hopkins LJ, Nugent E, Cox S, Glück IM, Tourlomousis P, et al. Inflammasome Activation Causes Dual Recruitment of NLRC4 and NLRP3 to the Same Macromolecular Complex. *Proc Natl Acad Sci USA* (2014) 111(20):7403–8. doi: 10.1073/pnas.1402911111
42. Franklin BS, Bossaller L, De Nardo D, Ratter JM, Stutz A, Engels G, et al. The Adaptor ASC has Extracellular and 'Prionoid' Activities That Propagate Inflammation. *Nat Immunol* (2014) 15(8):727–37. doi: 10.1038/ni.2913
43. Atianand MK, Harton JA. Uncoupling of Pyrin-Only Protein 2 (POP2)-Mediated Dual Regulation of NF- κ B and the Inflammasome. *J Biol Chem* (2011) 286(47):40536–47. doi: 10.1074/jbc.M111.274290
44. Zhou R, Tardivel A, Thorens B, Choi I, Tschopp J. Thioredoxin-Interacting Protein Links Oxidative Stress to Inflammasome Activation. *Nat Immunol* (2010) 11(2):136–40. doi: 10.1038/ni.1831
45. Erttmann SF, Gekara NO. Hydrogen Peroxide Release by Bacteria Suppresses Inflammasome-Dependent Innate Immunity. *Nat Commun* (2019) 10(1):3493. doi: 10.1038/s41467-019-11169-x
46. Salvesen GS, Dixit VM. Caspase Activation: The Induced-Proximity Model. *Proc Natl Acad Sci USA* (1999) 96(20):10964–7. doi: 10.1073/pnas.96.20.10964
47. Baroja-Mazo A, Martín-Sánchez F, Gomez AI, Martínez CM, Amores-Iniesta J, Compan V, et al. The NLRP3 Inflammasome Is Released as a Particulate Danger Signal That Amplifies the Inflammatory Response. *Nat Immunol* (2014) 15(8):738–48. doi: 10.1038/ni.2919
48. Van Gorp H, Saavedra PHV, de Vasconcelos NM, Opdenbosch NV, Vande Walle L, Matusiak M, et al. Familial Mediterranean Fever Mutations Lift the Obligatory Requirement for Microtubules in Pyrin Inflammasome Activation. *Proc Natl Acad Sci USA* (2016) 113(50):14384–9. doi: 10.1073/pnas.1613156113
49. Stein R, Kapplusch F, Heymann MC, Russ S, Staroske W, Hedrich CM, et al. Enzymatically Inactive Pro-caspase 1 Stabilizes the ASC Pyroptosome and Supports Pyroptosome Spreading During Cell Division. *J Biol Chem* (2016) 291(35):18419–29. doi: 10.1074/jbc.M116.718668

Conflict of Interest: The authors declare that the research was conducted in the absence of any commercial or financial relationships that could be construed as a potential conflict of interest.

Publisher's Note: All claims expressed in this article are solely those of the authors and do not necessarily represent those of their affiliated organizations, or those of the publisher, the editors and the reviewers. Any product that may be evaluated in this article, or claim that may be made by its manufacturer, is not guaranteed or endorsed by the publisher.

Copyright © 2021 Nagar, Rahman and Harton. This is an open-access article distributed under the terms of the Creative Commons Attribution License (CC BY). The use, distribution or reproduction in other forums is permitted, provided the original author(s) and the copyright owner(s) are credited and that the original publication in this journal is cited, in accordance with accepted academic practice. No use, distribution or reproduction is permitted which does not comply with these terms.